

# Langevin simulations of a model for ultrathin magnetic films

Lucas Nicolao\* and Daniel A. Stariolo†  
*Departamento de Física,  
Universidade Federal do Rio Grande do Sul  
CP 15051, 91501-979, Porto Alegre, Brazil‡*  
(Dated: December 2, 2024)

We show results from simulations of the Langevin dynamics of a two-dimensional scalar model with competing interactions for ultrathin magnetic films. We find a phase transition from a high temperature disordered phase to a low temperature phase with both positional and orientational orders. Both kinds of order emerge at the same temperature, probably due to the isotropy of the model Hamiltonian. In the low temperature phase orientational correlations show long range order while positional correlations show only quasi-long-range order in a wide temperature range. The orientational correlation length and the associated susceptibility seem to diverge with power laws at the transition. While at zero temperature the system exhibits stripe long range order, as temperature grows we observe the proliferation of different kinds of topological defects that ultimately drive the system to the disordered phase. The magnetic structures observed are similar to experimental results on ultrathin ferromagnetic films.

PACS numbers: 75.40.Mg, 75.40.Cx, 75.70.Kw

## I. INTRODUCTION

In the last years the interest in understanding the thermodynamic and mechanical properties of magnetic ultrathin films has grown considerably. Part of this interest is obviously motivated by the great amount of technological applications related to their magnetic behavior, such as data storage and electronics<sup>1</sup>. In recent years the advance in experimental techniques has made possible to study in great detail the complexity of magnetic order in thin films, where an extremely rich phenomenology is present<sup>2,3,4</sup>. Part of this phenomenology - as in many other physical and chemical systems<sup>5</sup> - is due to the presence of competing interactions acting on different length scales that frustrate the system and leads to mesoscopic pattern formation. In the case of an ultrathin magnetic film in the absence of an external magnetic field, stripe patterns of opposed magnetization are formed due to the competition between the ferromagnetic exchange interaction and the long-ranged dipolar interaction<sup>6</sup>.

Of particular interest for applications in data storage are films with perpendicular anisotropy, where spins point preferentially out of the plane. In the limit when the stripes width is much larger than the domain wall width, it is possible to replace the interaction between Heisenberg spins with a coarse-grained energy for the perpendicular component of the magnetization. Coarse-grained models of this kind have been studied in the past, but a complete phase diagram is still lacking. Theoretical analysis show a variety of possible scenarios, strongly dependent on the behavior of different kind of anisotropies<sup>6,7</sup>. Due to the intrinsic difficulty and approximate character of theoretical approaches, numerical simulations are essential in order to get a unified and coherent picture of the phenomenology. In an early work, Roland and Desai<sup>8</sup> studied the dynamical process of phase separation and emergence of stripe order

in Langevin simulations of a model for ultrathin films. More recently, Jagla<sup>4</sup> explored the different morphologies and patterns that can appear in such systems, showing a variety of very interesting phenomena. Nevertheless, up to our knowledge, more quantitative studies of the phase transitions and the different kinds of magnetic order present in these type of models have not been addressed up to now.

The aim of the present work is to study, by means of Langevin simulations of a coarse grained model of an ultrathin film, how thermal fluctuations affect the striped ground state order, the possible appearance of a phase transition at finite temperature, and the characterization of the magnetic structures relevant in each temperature region.

## II. MODEL AND NUMERICAL IMPLEMENTATION

The energy function of the model consists of both a local and a nonlocal terms:

$$H[\phi] = H_L[\phi] + H_{NL}[\phi] \quad (1)$$

The scalar field  $\phi(\mathbf{x})$  represents the out-of-plane component of the local magnetization, assuming preferentially two opposite values  $\pm\phi_0$ , according to the local potential:

$$H_L[\phi] = \frac{1}{2} \int d^2\mathbf{x} \left[ \kappa(\nabla\phi(\mathbf{x}))^2 - r\phi^2(\mathbf{x}) + \frac{u}{2}\phi^4(\mathbf{x}) \right] \quad (2)$$

In order that the local potential assume the desired double-well structure,  $u$  and  $r$  are taken to be positive phenomenological constants. The attractive square gradient term favors spatial homogeneity of the order parameter field.

The nonlocal term modeling a repulsive dipolar interaction has the form:

$$H_{NL}[\phi] = \frac{1}{2\delta} \int d^2\mathbf{x} \int d^2\mathbf{x}' \phi(\mathbf{x}) J(|\mathbf{x} - \mathbf{x}'|) \phi(\mathbf{x}') \quad (3)$$

where  $J(|\mathbf{x} - \mathbf{x}'|) = 1/|\mathbf{x} - \mathbf{x}'|^3$  in two dimensions, with the magnetic moments pointing perpendicular to the plane. In equations (2) and (3),  $\kappa$  and  $\delta$  are positive phenomenological constants that describe, respectively, the range of the short-range interaction and the strength of the long-range one. In all space integrations we assume a short distance cutoff  $2\pi/\Lambda$ , which in the numerical implementation appears naturally as the lattice constant  $a$ .

In the limit of strong damping, the relaxational dynamics of the system can be modeled by the following Langevin equations:

$$\frac{\partial\phi(\mathbf{x}, t)}{\partial t} = -\Gamma \frac{\delta H[\phi]}{\delta\phi(\mathbf{x}, t)} + \eta(\mathbf{x}, t) \quad (4)$$

where  $\Gamma$  is a constant (the mobility) which sets the time scale, and  $\eta(\mathbf{x}, t)$  is a Gaussian thermal noise with  $\langle\eta(\mathbf{x}, t)\rangle = 0$  and  $\langle\eta(\mathbf{x}, t)\eta(\mathbf{x}', t')\rangle = 2\Gamma T \delta(t-t') \delta^2(\mathbf{x} - \mathbf{x}')$ , as usual. Equation (4) can be explicitly written as:

$$\begin{aligned} \frac{\partial\phi(\mathbf{x}, t)}{\partial t} &= \kappa \nabla^2 \phi(\mathbf{x}, t) + r\phi(\mathbf{x}, t) - u\phi^3(\mathbf{x}, t) \\ &- \frac{1}{\delta} \int d^2\mathbf{x}' \phi(\mathbf{x}', t) J(|\mathbf{x} - \mathbf{x}'|) + \eta(\mathbf{x}, t) \end{aligned} \quad (5)$$

It is convenient to express the above equations in dimensionless form by means of the following transformations of the variables<sup>8</sup>:

$$\begin{aligned} \mathbf{x} &\rightarrow \left(\frac{r}{\kappa}\right)^{\frac{1}{2}} \mathbf{x} \\ \phi(\mathbf{x}, t) &\rightarrow \left(\frac{u}{r}\right)^{\frac{1}{2}} \phi(\mathbf{x}, t) \\ t &\rightarrow (\Gamma r) t, \end{aligned} \quad (6)$$

while the relevant parameters are renormalized as:

$$\delta = (\kappa r)^{\frac{1}{2}} \delta \quad (7)$$

$$T = \frac{u}{r\kappa} T \quad (8)$$

$$\Lambda = \left(\frac{\kappa}{r}\right)^{\frac{1}{2}} \Lambda \quad (9)$$

leading to the dimensionless form of equation (5):

$$\frac{\partial\phi(\mathbf{x}, t)}{\partial t} = \nabla^2 \phi(\mathbf{x}, t) + \phi(\mathbf{x}, t) - \phi^3(\mathbf{x}, t)$$

$$- \frac{1}{\delta} \int d^2\mathbf{x}' \phi(\mathbf{x}', t) J(|\mathbf{x} - \mathbf{x}'|) + \eta(\mathbf{x}, t) \quad (10)$$

with a short distance cutoff  $2\pi/\Lambda$  and thermal noise correlation  $\langle\eta(\mathbf{x}, t)\eta(\mathbf{x}', t')\rangle = 2T \delta(t-t') \delta^2(\mathbf{x} - \mathbf{x}')$ . Now the parameter  $\delta$  stands for the relative strength between the two competing interactions. The energy of the system (1) is renormalized in the same way as the temperature (8). The last Langevin equation can be written in Fourier space as:

$$\frac{\partial\phi(\mathbf{k}, t)}{\partial t} = -A(k)\phi(\mathbf{k}, t) + [-\phi^3(\mathbf{x}, t) + \eta(\mathbf{x}, t)]_{\mathbf{k}}^F \quad (11)$$

To be compatible with the subsequent numerical implementation of this equation, the last two terms were not explicitly written in Fourier space. Here  $]_{\mathbf{k}}^F$  means the  $\mathbf{k}$  component of the corresponding Fourier transform. The wave vector function  $A(k)$  corresponds to:

$$A(k) = k^2 - 1 + J(k)/\delta \quad (12)$$

which encodes all spatial information about the interactions. If this quantity has a negative minimum at a wave vector  $k_m$ , selected by varying  $\delta$ , the solution of equation (11) is a modulation in a single direction with periodicity given by  $k_m$ .

We have numerically solved the stochastic partial differential equation (11) discretizing space in a square lattice with mesh size  $a$ . Periodic boundary conditions were implemented using the Ewald summation technique<sup>9</sup> in the long-range dipolar interaction. After spatial discretization this interaction is no longer isotropic for all spatial scales and it becomes gradually anisotropic as the wave vector comes close to  $\pi$ . At the relevant spatial scales for our simulations,  $J(\mathbf{k})$  is slightly anisotropic.

We found it advantageous to use a spectral method, since in the Fourier space form of the Langevin equation (11) both spatial derivatives and the dipolar interactions acquire an algebraic form.

The time derivative was approximated using a simple Euler scheme with a time step  $\Delta t$ . Taking an isotropic form of the discretized laplacian, the spatial derivatives were treated using a semi-implicit method, where the  $k^2$  term in (11) is evaluated in the new time value. This treatment is standard to improve the stability of the algorithm<sup>10</sup>.

Therefore, discretizing equation (11) in such manner, i.e. through a first order semi-implicit spectral method, we obtain the following recurrence relation:

$$\phi(\mathbf{k}, t + \Delta t) = \frac{1}{1 + \Delta t k^2} \times \left\{ [1 + \Delta t - \Delta t a^2 J(\mathbf{k})/\delta] \phi(\mathbf{k}, t) + [-\Delta t \phi^3(\mathbf{x}, t) + \eta(\mathbf{x}, t)]_{\mathbf{k}}^F \right\} \quad (13)$$

After discretization the noise term  $\eta$ , in the way it appears in the last equation, is a random Gaussian number with amplitude  $(2T\Delta t/a^2)^{1/2}$ . The dipolar interaction  $J(\mathbf{k})$  in (13) is the fast Fourier transform of the result of the Ewald summation, evaluated at the beginning of the simulation.

The computational advantage of updating the system in Fourier space is accomplished using an adaptive FFT algorithm<sup>11</sup>, where the main time consuming operations are transforming Fourier the field  $\phi$  and the  $(-\phi^3 + \eta)$  term and then transforming back the new field value.

### III. RESULTS

We performed simulations of the continuum dipolar model through equation (13). We analyzed the case  $\delta = \sqrt{5}$ , where the ground state is a stripe modulated state with wave vector  $k_m = 1.01447$ , which is close to  $\pi/3$ . Simulations were performed for system sizes  $L = 192$  and  $L = 384$  for some temperatures.

The existence of a nontrivial solution with wave vector  $k_m$  of the Langevin equation (11) at zero temperature depends on whether the term in (12) is negative at  $k = k_m$ . Before the variables transformation (6), this could be done varying the parameter  $r$ . After the transformation, the existence of a solution is achieved tuning the mesh size  $a$ . We set  $a = \sqrt{5}$ .

The time integration was stable inside the range of temperatures we performed the simulations using a time step  $\Delta t = 0.5$ .

To measure the orientational order of the stripes we first consider the director field:

$$\hat{n}(\mathbf{x}) = \frac{\nabla\phi(\mathbf{x})}{|\nabla\phi(\mathbf{x})|} \quad (14)$$

which provides the local orientation of the stripe, when localized on a domain wall between opposite magnetizations. An analogy between this quantity and the Frank director of smectic liquid crystals has already been made on previous works<sup>12,13,14</sup>, and leads to the definition of a tensor order parameter:

$$Q_{\alpha\beta}(\mathbf{x}) = n_\alpha(\mathbf{x})n_\beta(\mathbf{x}) - \frac{1}{2}\delta_{\alpha\beta} \quad (15)$$

where  $\alpha, \beta = 1, 2$  are the cartesian components. Similar to a nematic order parameter in a liquid crystal, an orientational order parameter  $Q$  can be defined as the positive eigenvalue of the spatial average of the above tensor order parameter<sup>15</sup>. This value corresponds to the quantity  $\cos 2\theta$ , where  $\hat{n} = (\cos \theta, \sin \theta)$  and  $\theta$  is the angle between the local director field and the mean orientation of the system. But, since the director field inside the stripe domains does not necessarily provide the local orientation of the stripe, to get a more precise value for the orientational order parameter we average Eq.(15) only over

domain wall sites, namely:

$$\bar{Q}_{\alpha\beta} = \frac{1}{L'} \sum'_{\mathbf{x}} Q_{\alpha\beta}(\mathbf{x}) \quad (16)$$

where the prime denotes the restricted sum with  $L'$  being the total number of domain wall sites. Now we can write explicitly the orientational order parameter as:

$$Q = \sqrt{\bar{Q}_{11}^2 + \bar{Q}_{12}^2} \quad (17)$$

One possible way to characterize the positional order of the stripes is through a staggered magnetization, defined as:

$$m_{\mathbf{k}} = \left\langle \frac{1}{L^2} \sum_{\mathbf{x}} \text{sgn}(\phi(\mathbf{x})) \text{sgn}(\cos(\mathbf{k} \cdot \mathbf{x})) \right\rangle \quad (18)$$

where  $\text{sgn}$  is the sign function and for  $\mathbf{k}$  we use the ground state wave vector.

The results we present here were obtained with the following procedure: the system is initialized in the ground state and heated with a heating rate  $d_T$ . At each temperature of interest, the heating process is halted and the system is left to run a transient period of  $n_t$  time steps before we start recording system configurations at each  $n_m$  time steps, used later to measure the desired quantities. Typical values of  $n_t$  were between  $5 \times 10^4$  to  $4 \times 10^6$  in order to get as close as possible to equilibrium. For temperatures away from criticality we checked different values of  $n_t$  in order to get stationary mean values of the order parameters. Typical  $n_m$  values were in the order of  $10^5$  and the results are averages over 20 to 60 system configurations.

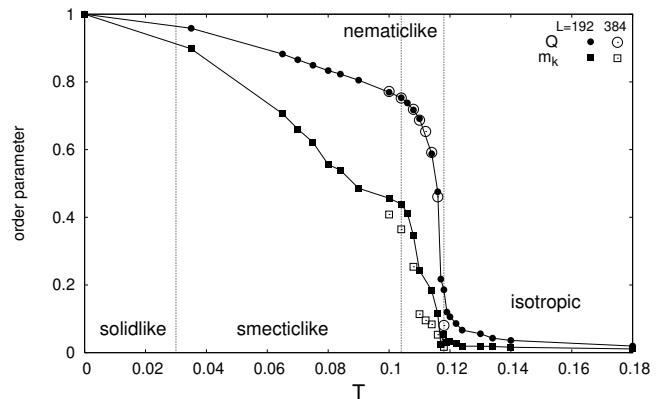


FIG. 1: Order parameters as a function of temperature for  $L = 192$ . The open symbols corresponds to the larger system size,  $L = 384$ . Thin vertical lines separate approximately temperature ranges of the different regimes.

In Fig.(1) we show the results for the positional and orientational order parameters. The data clearly shows a phase transition, where both kinds of order emerge at a finite temperature. In the  $L = 192$  case we found that

the two order parameters decay simultaneously to zero at  $T \approx 0.12$ , even though the staggered magnetization drops significantly at  $T = 0.11$ . In the region in between the positional order parameter seems to present strong finite size effects. As the temperature is lowered in the ordered phase, a stripe structure develops gradually by the annihilation of defects (see Fig.(3)). Although we were unable to study in more detail the finite size scaling near the transition, it seems improbable that an intermediate, nematic-like phase, with only orientational order can be present in this model. Although positional order decays faster than the orientational one, our results point to the presence of a single phase transition from a disordered high temperature phase to a low temperature phase with both orientational and translational orders. This is one of the possible scenarios that emerge from a theoretical analysis of a similar model by Abanov et al.<sup>7</sup>.

To take a closer look at the structural properties of the different magnetic configurations, we calculated the static structure factor:

$$S(\mathbf{k}) \equiv \left\langle |\phi(\mathbf{k})|^2 \right\rangle \quad (19)$$

and the associated spatial correlation function, given by:

$$C(\mathbf{r}) = \frac{1}{L^2} \sum_{\mathbf{k}} e^{i\mathbf{r} \cdot \mathbf{k}} S(\mathbf{k}), \quad (20)$$

that can be quickly computed using a fast Fourier transform<sup>11</sup>. The relevant directions for the spatial correlation function are the directions parallel and perpendicular to the stripes, respectively denoted by  $C_x$  and  $C_y$ . These quantities describe the positional order along the two relevant directions. We have also computed nematic (or orientational) correlation functions<sup>13,14</sup>, since they encode information on the spatial decay of orientational order of the stripes. Nematic correlations are defined as:

$$\begin{aligned} C_{nn}(\mathbf{r}) &= \frac{2}{L^2} \sum_{\mathbf{x}} \langle \text{Tr} Q(\mathbf{x} + \mathbf{r}) Q(\mathbf{x}) \rangle \quad (21) \\ &= \frac{1}{L^2} \sum_{\mathbf{x}} \langle Q_{11}(\mathbf{x} + \mathbf{r}) Q_{11}(\mathbf{x}) \\ &\quad + Q_{12}(\mathbf{x} + \mathbf{r}) Q_{12}(\mathbf{x}) \rangle \quad (22) \end{aligned}$$

where the function summed up in Eq. (21) is analogous to  $\langle \cos [2\theta(\mathbf{x} + \mathbf{r}) - 2\theta(\mathbf{x})] \rangle$ . Examples of positional and orientational correlation functions can be seen in Figures (2) and (4) for two different temperatures.

For low enough temperatures ( $T < 0.11$ ), the nematic correlations are strongly affected by residual oscillations of the field  $\phi(\mathbf{x})$ . In order to obtain accurate values for the orientational correlation function we found convenient to smooth the tensor order parameter (15) following a smoothing procedure introduced in Ref.<sup>14</sup>. We smooth the fields  $Q_{11}(\mathbf{x})$  and  $Q_{12}(\mathbf{x})$  using for each the iterative

process:

$$f_{(n+1)}(\mathbf{x}) = \frac{1}{2} f_{(n)}(\mathbf{x}) + \frac{1}{8} \sum_{\mathbf{x}' \in NN} f_{(n)}(\mathbf{x}') \quad (23)$$

where  $f_{(n)}$  is one of the fields after  $n$  iterations, and  $NN$  means the four nearest neighbors of  $\mathbf{x}$  on the square lattice. We found that three iterations are enough to get sensible results (see Fig.(2)). Similar smoothing procedures for orientational correlation functions were used in simulations of melting of two-dimensional solid systems<sup>16,17</sup>. For clarity, in this work we always show the connected orientational correlation function, where the mean square orientational order parameter is subtracted from Eq.(22). In this way,  $C_{nn}$  accounts for direction fluctuations only.

At sufficiently low temperatures ( $T < 0.03$ ) spatial correlations decay immediately to a constant and there is positional and orientational long-range order (see Fig.(1) for the values of the order parameters in the corresponding temperature regimes).

At slightly higher temperature and in a wide range ( $0.03 < T < 0.11$ ) we found evidence of a low temperature smectic-like regime, similar to the smectic crystal phase predicted by Abanov et al.<sup>7</sup> and observed experimentally by Portmann et al.<sup>2</sup>. In this phase, phonon-like fluctuations (meandering excitations) alone are sufficient to cause algebraic decay of positional correlations at low temperatures for  $T > 0.03$ . But at  $T = 0.09$  bound pairs of dislocations appear and become more common as temperature increases. Long-range *orientational* order persists over a wider range of temperatures, but above  $T = 0.065$  orientational order also starts to decay algebraically.

An example of the algebraic behavior of the correlation functions in this region is shown in Fig.(2) for  $T = 0.1$ . It is important to note that the exponent of the positional algebraic decay in this regime increases with temperature and is different in the perpendicular and parallel directions - exponents values range from  $\omega_x = 0.034$  and  $\omega_y = 0.036$  for  $T = 0.035$  to  $\omega_x = 0.365$  and  $\omega_y = 0.212$  for  $T = 0.104$ . As for the orientational order we observe a small temperature dependence of the algebraic decay exponent in the perpendicular direction, with exponents lying in the range  $1.18 < \alpha < 1.43$ . In the parallel direction, the orientational correlation function is a constant, indicating long-range order in this direction.

In Fig.(3) we illustrate some typical configurations of this phase. We see that it is characterized by phonon-like excitations and a finite density of dislocation pairs - some different types are shown encircled.

In a narrow range of temperatures,  $0.11 < T < 0.118$ , where the orientational order parameter is still high but the staggered magnetization drops considerably fast, we found a change of behavior in the correlation functions. In the parallel direction, positional order is decorrelated exponentially rapidly to zero, indicating absence of translational order of the stripes. In the perpendicular direction, where order is more robust, there is an intermediate

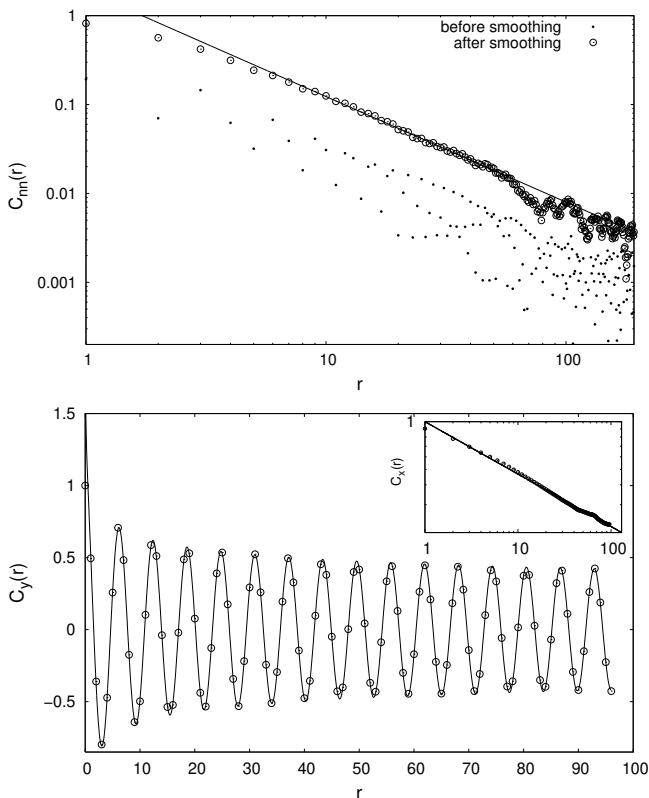


FIG. 2: Correlation functions in the smectic-like region at  $T = 0.1$ . The upper figure shows the connected orientational correlation function in the perpendicular direction for  $L = 384$ , plotted in log-log scale, before and after the smoothing procedure. The continuous line corresponds to a fitting by the function  $A r^{-\alpha_y}$ , with  $\alpha_y = 1.18$  and  $A$  a fitting parameter. In the parallel direction this function decays immediately to zero. The lower figure shows the parallel (inset) and perpendicular spatial correlations functions, both for  $L = 192$ . The parallel  $C_x$  function is plotted in a log-log scale. The continuous lines corresponds to fittings by the functions  $r^{-\omega_x}$  and  $\cos(k_0 r) r^{-\omega_y}$  with  $\omega_x = 0.33$  and  $\omega_y = 0.19$  and  $k_0 = 1.014$ . Similar values were found in the  $L = 384$  case.

kind of behavior where the positional correlation function is better fitted by a product of a power law and an exponential. An example of this behavior is shown in Fig.(4), where one can also see that the connected orientational correlation functions now decay exponentially in both directions but with different correlation lengths. Orientational domains in this regime are larger in the perpendicular direction.

Analyzing visually the configurations of this region we observe many excitations disrupting orientational order. A typical configuration is shown in Fig.(5). We see that this regime presents large Burgers vector dislocations that can be regarded as a tightly-bound pair of oppositely charged disclinations<sup>12</sup>. There are also what may be called a dislocation cascade, a series of bifurcations within a single stripe (colored in Fig.(5a)). Small domains of perpendicular orientation (encircled in Fig.(5a))

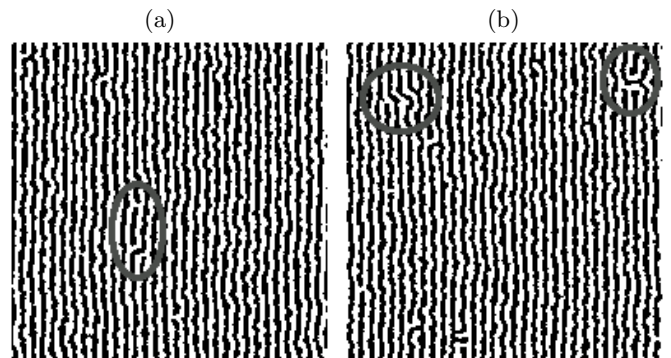


FIG. 3: Typical configurations in the smectic phase for  $L = 192$  at (a)  $T = 0.1$  and (b)  $T = 0.104$ . In (a) the encircled region exhibits two pairs of dislocations; above there is a "passage" due to two dislocations inserted in the same stripe, and below a pair of dislocations separated by one stripe. In (b) a pair separated by four stripes and a pair formed by a larger Burgers vector dislocation and a double dislocation.

are present as well, and become more common and larger as temperature increases (see Fig.(5b)). Surrounded by topological defects there are domains of locally smectic-like arranged stripes, where order is decorrelated mainly by meandering excitations and all kinds of pairs of dislocations (some are encircled in Fig.(5a)).

In order to estimate the transition temperature  $T_c$  between the orientationally ordered and isotropic phases, we have measured the orientational correlation length and susceptibility of  $Q$  in the isotropic phase. The results for  $L = 192$  are shown in Fig. (6), together with power-law fits. We found that  $T_c$  lies close to  $T_c \approx 0.117$  and that divergences are well fitted by power-law forms, at variance with the exponential divergence that one would expect in a defect-mediated transition according to the KTHNY theory<sup>12,16</sup>. The power law behavior seems to be in agreement with a recent result in which the nematic transition is predicted to be second order<sup>18</sup>.

Finally, we discuss the evolution of the structure factor, eq.(19), with temperature. In Fig.(7) we show four characteristic examples around the transition. From the first to the second plot it can be seen that the sharp peaks characterizing stripe order are replaced by nematic-like peaks, spreaded along the ring  $|\mathbf{k}| = k_m$  due to angle fluctuations. The transition to the disordered phase seems to be through an increase of domains of perpendicular orientation of the stripes. In the structure factor, this is reflected as the growth of two symmetric peaks around  $k \approx k_m$  in the perpendicular direction. Immediately after the transition, at  $T = 0.118$ , the four symmetrical peaks are equivalent, as can be seen in the third plot. As the temperature is further increased, angle fluctuations around this two preferential directions smear out the four peaks and the system becomes almost isotropic and the spectral weight of the structure factor lies on a ring with a weakly tetragonal shape, as shown in Fig. 6. A typical configuration illustrating the weakly tetragonal symme-

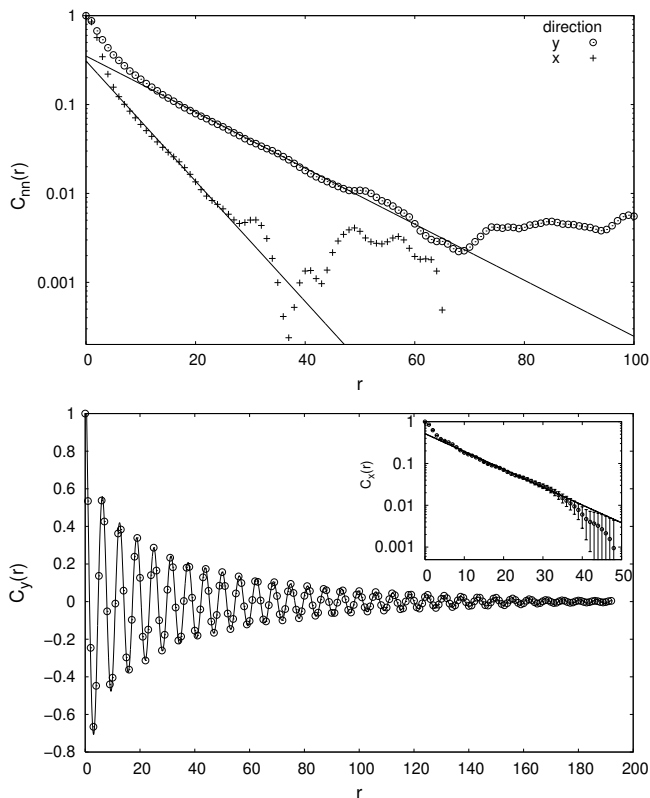


FIG. 4: Correlation functions in the nematic-like region at  $T = 0.114$  and  $L = 384$ . The upper figure shows the connected orientational correlation function in the perpendicular and parallel directions in a log-linear scale. The continuous lines corresponds to fittings by the function  $A \exp(-r/\lambda)$ , with  $\lambda_y = 13.77$  and  $\lambda_x = 6.42$ . The lower figure shows the parallel (inset) and perpendicular spatial correlations functions. The parallel  $C_x$  function is plotted in a log-linear scale. The continuous lines correspond to fittings by the functions  $A \exp(-r/\xi_x)$  and  $\cos(k_0 r) \exp(-r/\xi_y) r^{-\omega_y}$  with  $\xi_x = 10.17$  and  $\xi_y = 60.0$  and  $\omega_y = 0.26$  and  $k_0 = 0.98$ .

try of the disordered phase just above the transition is shown in Fig. 8.

Not far away from the transition, the isotropic phase still presents the exponential-algebraic behavior of positions correlations as in the nematic-like regime, indicating that it locally resembles the low temperature phase. The anisotropic feature of the orientational correlation function disappears in this phase, where  $C_{nn}$  decays exponentially to zero.

#### IV. CONCLUSIONS

We have made Langevin simulations at finite temperature of a model for ultrathin ferromagnetic films with perpendicular anisotropy. These systems have a stripe ground state due to competition between exchange and dipolar interactions. We have found a phase transition from a high temperature disordered phase to a low tem-

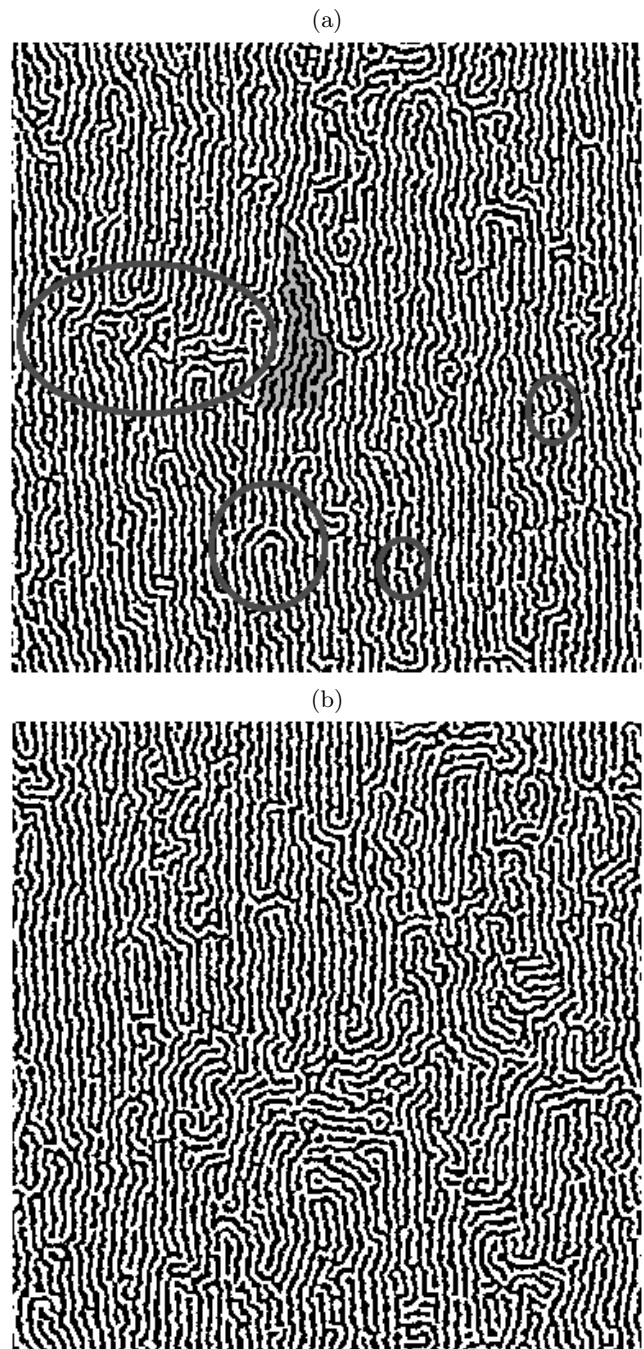


FIG. 5: Typical configuration in the nematic-like region at (a)  $T = 0.114$  and (b)  $T = 0.116$  for  $L = 384$ . In (a) some defects are put in evidence. In small circles, two pairs of dislocations inside smectic-like domains; in the larger circle a disclination dipole; shown colored a series of dislocations inside a single stripe and in an ellipse a domain of perpendicular orientation.

perature phase with both positional and orientational orders. Below the transition point isotropy is spontaneously broken, and a smectic-like magnetic structure develops. Both kinds of ordering seem to take place at the same  $T_c$ , in agreement with some previous theoretical predictions. The absence of an intermediate, purely ori-

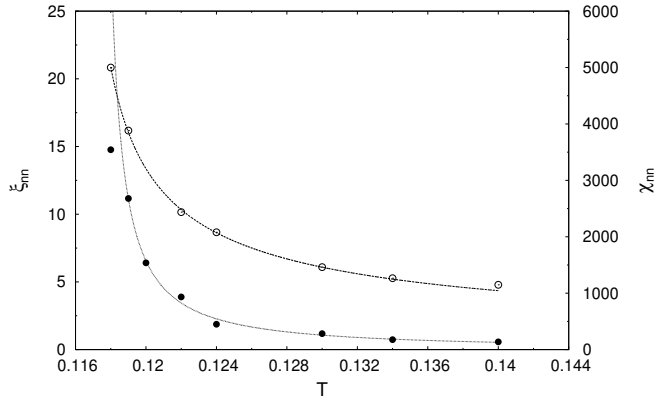


FIG. 6: Orientational correlation length (full symbols) and susceptibility (open symbols) as a function of temperature in the isotropic phase. The continuous curves show power-law fittings, namely:  $\xi_{nn}(T) \sim (T - 0.1172)^{-1.19}$  and  $\chi_{nn}(T) \sim (T - 0.1161)^{-0.61}$ .

entational, phase is probably due to the isotropic nature of the model Hamiltonian. Other terms, which explicitly break orientational order, may be necessary in order to have an intermediate nematic phase. This is what emerges from a recent analysis of the nematic transition in this same model, where an extra term was included and shown to be responsible for the existence of an intermediate nematic phase<sup>18</sup>. The nature of these terms depend on microscopic interactions, namely, on the modelling of the anisotropy contribution. In this respect, more input from experiments is fundamental.

We have found that the numerical results show complex magnetic structures, with positional and orientational correlations decaying algebraically at low temperatures. Positional correlations have different exponents for the longitudinal and perpendicular components, relative to the ground state stripe orientation. The exponents are also temperature dependent. In the case of orientational correlations, we observe a weak temperature dependence in the perpendicular direction, and a saturation to a constant value in the longitudinal direction. Qualitatively one can say that we observe positional quasi-long-range order and orientational long range order, at low temperatures.

As temperature grows it is possible to observe a proliferation of topological defects, with structures similar to those observed in real systems. In a narrow region around the transition temperature, both positional and orientational correlations begin to decay exponentially. A power law fit of the data of the orientational correlation length and the associated susceptibility in the high temperature region allows us to estimate the critical temperature. This power law dependence of the orientational correlation length does not agree with the well known KTHNY theory of two dimensional melting. We do not know to what extent the predictions from this theory should be applicable to magnetic two dimensional sys-

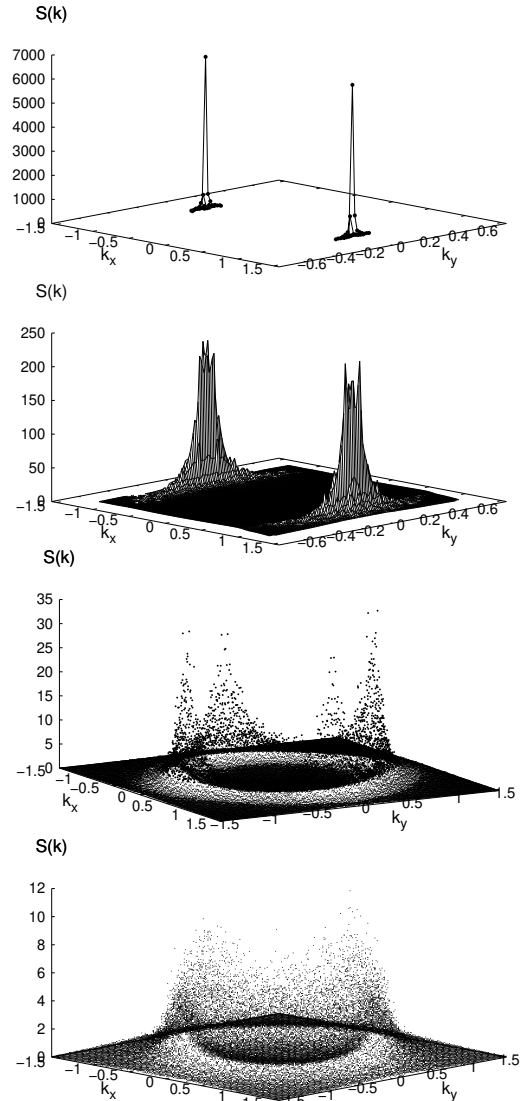


FIG. 7: Structure factor at  $T = 0.1, 0.114, 0.118$  and  $0.14$  for  $L = 384$ .

tems like this. Our results are in agreement with a possible scenario for a smectic magnetic system put forward by Abanov and coworkers more than 10 years ago<sup>7</sup>, and with a recent result on the second order nature of the nematic transition in the same model studied in this work supplemented by another term in the Hamiltonian which explicitly breaks orientational order<sup>18</sup>.

We found that the weak anisotropy of the dipolar interaction due to spatial discretization and the short width of the stripes (of three grid points) has led to a pinning effect that favored the stripes orientation to be preferentially on the two Cartesian directions. But looking at the structure factor around the transition, we found that the fluctuations responsible for disrupting orientational

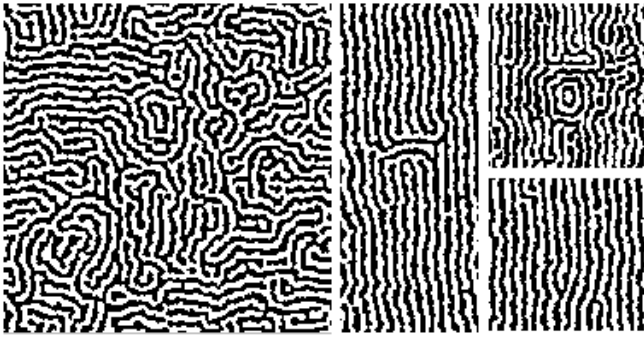


FIG. 8: The left configuration shows the isotropic phase at  $T = 0.12$  for  $L = 192$ , presenting a target defect close to its center. Small target defects are ubiquitous in this phase. At top right we show a large target defect in a portion of a  $L = 480$  configuration in an out-of-equilibrium disordering process at  $T = 0.13$ . In the middle a portion of a  $L = 384$  configuration at  $T = 0.112$  exhibiting a large dislocation pair made of disclination pairs. Below, pairs of dislocations at  $T = 0.104$ .

order are not restricted to the two Cartesian directions and the isotropic nature of the model still manifests.

More quantitative analytic predictions are clearly needed in order to assess the quality and limitations of

our results. Also, it would be extremely interesting to do systematic experimental measurements of structure factors and correlations as a function of temperature, like the ones done by Pescia and coworkers<sup>2,19,20</sup>. This would allow, between other things, to elucidate the experimental conditions under which a nematic intermediate phase can be present in a magnetic system. The similarity between our simulations and experimental images of perpendicularly magnetized fcc Fe films grown on Cu(100)<sup>2,19,20</sup> is striking. For example, target defects first observed by Vaterlaus *et al.*<sup>19</sup> were observed in our simulations and are ubiquitous in the disordered phase (see Fig.(8)).

Finally, the dynamical behavior of these systems also deserve to be studied, because the presence of frustration and the emergence of many kinds of topological defects lead to a complex dynamics, with pinning of magnetic structures during long time scales, before the final, asymptotic equilibrium state sets in<sup>21</sup>.

The “*Conselho Nacional de Desenvolvimento Científico e Tecnológico CNPq-Brazil*” is acknowledged for financial support. DAS also wants to acknowledge the Abdus Salam International Centre for Theoretical Physics for financial support to the *Latinamerican Network on Slow Dynamics in Complex Systems* through grant NET-61.

---

\* Electronic address: nicolao@if.ufrgs.br  
 † Electronic address: stariolo@if.ufrgs.br  
 ‡ Research Associate of the Abdus Salam International Centre for Theoretical Physics, Trieste, Italy  
<sup>1</sup> A. Hubert and R. Schafer, *Magnetic Domains* (Springer-Verlag, Berlin, 1998).  
<sup>2</sup> O. Portmann, A. Vaterlaus, and D. Pescia, *Nature* **422**, 701 (2003).  
<sup>3</sup> Y. Wu, C. Won, A. Scholl, A. Doran, H. Zhao, X. Jin, and Z. Qiu, *Physical Review Letters* **93**, 117205 (2004).  
<sup>4</sup> E. A. Jagla, *Phys. Rev. E* **70**, 046204 (2004).  
<sup>5</sup> M. Seul and D. Andelman, *Science* **267**, 476 (1995).  
<sup>6</sup> T. Garel and S. Doniach, *Phys. Rev. B* **26**, 325 (1982).  
<sup>7</sup> A. Abanov, V. Kalatsky, V. L. Pokrovsky, and W. M. Saslow, *Phys. Rev. B* **51**, 1023 (1995).  
<sup>8</sup> C. Roland and R. Desai, *Phys. Rev. B* **42**, 6658 (1990).  
<sup>9</sup> D. Frenkel and B. Smith, *Understanding Molecular Simulation* (Academic Press, New York, 1996).  
<sup>10</sup> W. H. Press, S. A. Teukolsky, W. T. Vetterling, and B. P. Flannery, *Numerical Recipes* (Cambridge University Press,

1992).  
<sup>11</sup> M. Frigo and S. G. Johnson, in *Proceedings of the IEEE* (2005), vol. 93, p. 216.  
<sup>12</sup> J. Toner and D. R. Nelson, *Phys. Rev. B* **23**, 316 (1981).  
<sup>13</sup> J. J. Christensen and A. J. Bray, *Phys. Rev. E* **58**, 5364 (1998).  
<sup>14</sup> H. Qian and G. F. Mazenko, *Phys. Rev. E* **67**, 036102 (2003).  
<sup>15</sup> J. A. Cuesta and D. Frenkel, *Phys. Rev. A* **42**, 2126 (1990).  
<sup>16</sup> S. Z. Lin, B. Zheng, and S. Trimper, *Phys. Rev. E* **73**, 066106 (2006).  
<sup>17</sup> A. Jaster, *Phys. Rev. E* **59**, 2594 (1999).  
<sup>18</sup> D. G. Barci and D. A. Stariolo, preprint cond-mat/0611364.  
<sup>19</sup> A. Vaterlaus, C. Stamm, U. Maier, M. G. Pini, P. Politi, and D. Pescia, *Phys. Rev. Lett.* **84**, 2247 (2000).  
<sup>20</sup> O. Portmann, A. Vaterlaus, and D. Pescia, *Phys. Rev. Lett.* **96**, 047212 (2006).  
<sup>21</sup> R. Mulet and D. A. Stariolo, preprint cond-mat/0607185.